ORIGINAL LABORATORY RESEARCH REPORT

OPEN

Novel Opioid Analgesics for the Development of Transdermal Opioid Patches That Possess Morphine-Like Pharmacological Profiles Rather Than Fentanyl: Possible Opioid Switching Alternatives Among Patch Formula

Akane Komatsu, MD,*† Kanako Miyano, PhD,†‡ Daisuke Nakayama, PhD,§ Yusuke Mizobuchi, MD,†‡‖ Eiko Uezono, MD,†¶ Kaori Ohshima, MS,† Yusuke Karasawa, MS,†¶ Yui Kuroda, MD,*† Miki Nonaka, PhD,* Keisuke Yamaguchi, MD, PhD,¶ Masako Iseki, MD, PhD,*¶ Yasuhito Uezono, MD, PhD,†¶# and Masakazu Hayashida, MD, PhD*¶

BACKGROUND: Transdermal fentanyl is widely used in the treatment of severe pain because of convenience, safety, and stable blood concentrations. Nevertheless, patients often develop tolerance to fentanyl, necessitating the use of other opioids; transdermal buprenorphine patch is widely used as an analgesic agent, though available formulation does not provide comparable analgesic effect as transdermal fentanyl patch. Opioids bind to the opioid receptor (OR) to activate both G protein–mediated and β-arrestin–mediated pathways. We synthesized morphine-related compounds with high transdermal absorbability (N1 and N2) and evaluated their OR activities pharmacologically in comparison with fentanyl and morphine.

METHODS: In cells stably expressing μ-opioid receptor (MOR), δ-opioid receptor (DOR), and κ-opioid receptor (KOR), G protein–mediated pathways were assessed using the CellKey and an intracellular cyclic adenosine monophosphate (cAMP) assay, while β-arrestin–mediated pathways were analyzed with β-arrestin recruitment and receptor internalization assays. Furthermore, analgesic effects were evaluated using a tail-flick test in mice, and the analgesic effect on fentanyl-tolerant mice was evaluated.

RESULTS: In the CellKey and cAMP assays, both N1 and N2 showed the highest affinity for MOR and acted as full agonists as well as partial agonists for DOR and KOR. In the β-arrestin and internalization assays, only fentanyl acted as a full agonist; N1 and N2 acted as partial agonists of MOR. In the mouse tail-flick test, N1 and N2 showed analgesic effects equivalent to those of fentanyl and morphine. In fentanyl-tolerant mice, fentanyl showed a diminished analgesic effect, whereas N1 and N2 as well as morphine retained their analgesic effects.

CONCLUSIONS: While N1 and N2 have higher transdermal absorbability than fentanyl, they also have analgesic effects comparable to those of morphine, suggesting that they may be attractive compounds for the development of novel opioid patches for transitioning from fentanyl patches. (Anesth Analg 2022;134:1082–93)

KEY POINTS

- **Question:** Are there novel opioid analgesics potentially suitable for patch formulation for transitioning from transdermal fentanyl?
- **Findings:** We synthesized novel opioids new-opioid 1 (N1) and new-opioid 2 (N2), which possess morphine-like pharmacological profiles with transdermal activity, and they showed fewer tolerance characteristics in fentanyl-tolerant mice.
- **Meaning:** Analgesics, such as N1 and N2, could serve as novel transdermal opioids for transitioning from fentanyl patches.

GLOSSARY

ANOVA = analysis of variance; **AUC** = area under the curve; **BSA** = bovine serum albumin; **cAMP** = cyclic adenosine monophosphate; **CHO-K1 OPRD1** = Chinese hamster ovary expressing δ-opioid receptor; **CHO-K1** = Chinese hamster ovary expressing κ-opioid receptor; **CRF-1** = Charles River formula-1; **DAMGO** = D-Ala(2)-N-Me-Phe(4)-Glyol(5)-enkephalin; **DOR** = δ-opioid receptor; **GPCR** = G protein-coupled receptor; **HEK293** = human embryonic kidney 293; **HEPES** = 4-(2-hydroxyethyl)-1-piperazineethanesulfonic acid; **IBMX** = 3-isobutyl-1-methylxanthine; **KOR** = κ-opioid receptor; **MOR** = μ-opioid receptor; **n.d** = not detected; **N1** = new opioid 1; **N2** = new opioid 2; **ns** = not significant; **ORs** = opioid receptors; **pGS22F** = pGlosensorTM-22F plasmid; **SEM** = standard error of mean; **SNC80** = (+)-4-[(aR)-a-((2S,5R)-4-allyl-2,5-dimethyl-1-piperazinyl)-3-methoxybenzyl]-N,N-diethylbenzamide; **U2OS OPRK1** = human bone osteosarcoma U2OS expressing κ-opioid receptor; **U2OS OPRM1** = human bone osteosarcoma U2OS expressing μ-opioid receptor; **U-50488H** = trans3,4-dichloro-N-methyl-N[2(pyrrolidinyl)-cyclohexyl]-benzeneacetamide; **WHO** = World Health Organization

A recent review of the pharmacological management of cancer pain reported that 70% of cancer patients experience acute or chronic cancer pain, manifesting as physical pain with psychological and social effects that significantly reduce quality of life.[1–5] Approximately 80% of cancer pain is now controlled with the proper use of analgesics[6]; pain is generally managed according to the World Health Organization (WHO) pain ladder, and potent opioids are typically used.[7] Fentanyl, morphine, oxycodone, and hydromorphone are commonly used according to the patients' pain condition.[7] Among these analgesics, fentanyl patches are widely used because they require no administration devices, offer safety and convenience, avoid the first-pass effect, and are slowly absorbed to maintain the required blood concentrations.[8,9] However, use of these patches is associated with tolerance, often necessitating a transition to other opioids.[10–13] Unfortunately, morphine, oxycodone, and hydromorphone have poor transdermal absorption, and there are currently no alternative potent opioid patches to substitute for transdermal fentanyl. Thus, the development of novel opioid patch formulations is essential.

Opioid receptors (ORs) are classified into 3 subtypes—μ opioid receptor (MOR), δ opioid receptor (DOR), and κ opioid receptor (KOR)—and analgesic effects are mainly mediated by MOR.[14,15] ORs belong to the G protein-coupled receptor (GPCR) family, which conjugate with Gi/o proteins and cause a decrease in intracellular cyclic adenosine monophosphate (cAMP) levels.[14,16] Cellular activities mediated by ORs are transduced through 2 pathways: the G protein–mediated pathway, which is involved mainly in analgesia, and the β-arrestin–mediated pathway, which is related to adverse effects.[14–20] Accordingly, novel drugs that activate the G protein–mediated pathway without activating the β-arrestin–mediated pathway are expected to be effective analgesics.

Therefore, we aimed to develop novel opioids that could be used in patch formulations for patients switching from fentanyl patches. To this end, we synthesized 2 novel compounds, namely N1 (new opioid 1) and N2 (new opioid 2), that showed good transdermal permeability and that were expected to have MOR potencies similar to that of morphine. We evaluated their effects on ORs by comparing their properties with those of morphine and fentanyl in vitro and in vivo. We then analyzed the effects of N1 and N2 on OR activities in both G protein–mediated and β-arrestin–mediated pathways using in vitro assays. We further examined the analgesic effects of N1 and N2 by using in vivo assays in mice.

METHODS

All experiments were approved and performed in accordance with the Guide for Genetic Modification Safety Committee, National Cancer Center, Japan (approval no. B85M1-17). Animal experiments were conducted in accordance with the ethical guidelines of the International Association for the Study of Pain and were approved by the Committee for Ethics of Animal Experimentation of Daiichi Sankyo Co, Ltd (approval no. A1601802).

Evaluation of the Cutaneous Permeability of N1 and N2

The skin permeation rate was measured using a horizontal diffusion cell (PermeGear).[21,22] All test compounds were dissolved in 3.84 mM isopropyl myristate. We used the β2 adrenergic receptor agonist tulobuterol as a percutaneous positive control.[23] Skin samples were isolated from hairless mice (HR-1 strain, male, 7 weeks of age; Japan SLC), punched out to a diameter of 24 mm, and sandwiched between horizontal diffusion cells. Three skin pieces were taken from a mouse, and each test compound (tulobuterol, N1, and N2) was treated, respectively. The horizontal diffusion cells were maintained at 37 °C in a circulating constant-temperature water bath. We added 0.9 mL of McIlvaine buffer containing 40% polyethylene glycol 400 to the dermal surface (receiver side), and 0.9 mL of each test compound solution (donor solution) to the stratum corneum surface (donor side). After applying the donor solution, the same amount

From the *Department of Anesthesiology and Pain Medicine, Juntendo University Graduate School of Medicine, Tokyo, Japan; †Department of Pain Control Research, The Jikei University School of Medicine, Tokyo, Japan; ‡Division of Cancer Pathophysiology, National Cancer Center Research Institute, Tokyo, Japan; §Daiichi Sankyo Company, Limited, Nihonbashihonmachi, Tokyo, Japan; ‖Department of Anesthesiology and Resuscitology, Okayama University Graduate School of Medicine, Dentistry, and Pharmaceutical Sciences, Okayama, Japan; ¶Department of Pain Medicine, Juntendo University Graduate School of Medicine, Bunkyo-ku, Japan; and #Supportive and Palliative Care Research Support Office, National Cancer Center Hospital East, Chiba, Japan.

Accepted for publication January 6, 2022.

Funding: This study was supported in part by Grants-in-Aid for Scientific Research (KAKENHI) from the Japan Society for the Promotion of Science (JSPS) Grant Numbers JP18K07404 and JP18K08858; the National Cancer Center Research and Development Fund (29-S-5); and a grant from Daiichi Sankyo Company, Limited.

Conflicts of Interest: See Disclosures at the end of the article.

Supplemental digital content is available for this article. Direct URL citations appear in the printed text and are provided in the HTML and PDF versions of this article on the journal's website (www.anesthesia-analgesia.org).

Reprints will not be available from the authors.

Address correspondence to Yasuhito Uezono, MD, PhD, Department of Pain Control Research, The Jikei University School of Medicine, 3-25-8, Nishi-Shimbashi, Minato-ku, Tokyo 105-8461, Japan. Address e-mail to yuezono@jikei.ac.jp.

DOI: 10.1213/ANE.0000000000005954

of new receiver solution was added. The content of the test compounds in the collected receiver solution was analyzed, and the skin permeation rate (flux, $\mu g \cdot cm^{-2} \cdot h^{-1}$) was calculated. The repeatability of each compound was measured in 3 independent mice.

Construction of Plasmids and Generation of Stable Cell Lines

Construction of plasmids and generation of stable cell lines for MOR have been described previously.[17] Halotag fused DOR or KOR (Halotag DOR or Halotag KOR, Kazusa DNA Research Institute) with the pGlosensor-22F plasmid (pGS22F; Promega Corp) was amplified according to the manufacturer's instructions. Human embryonic kidney 293 (HEK293) cells (ATCC) and HEK293 cells stably expressing Halotag MOR, Halotag DOR, and Halotag KOR without pGS22F were generated by transfection of the constructed plasmids using Lipofectamine reagent (Life Technologies Corp). These were selected based on OR activity measured using the CellKey assay or the Glosensor cAMP assay.

Cell Culture

HEK293 cells stably expressing Halotag MOR/pGS22F, Halotag DOR/pGS22F, or Halotag KOR/pGS22F were cultured in DMEM supplemented with 10% fetal bovine serum albumin (BSA), penicillin (100 U/mL), streptomycin (100 mg/mL), and 5 μg/mL puromycin (InvivoGen) and 100 μg/mL hygromycin (FUJIFILM Wako Pure Chemical Corporation) for Halotag MOR/pGS22F, and 700 μg/mL genistein (Glico) and 100 μg/mL hygromycin for Halotag DOR/pGS22F and Halotag KOR/pGS22F, in a humidified atmosphere containing 95% air and 5% CO_2 at 37 °C.

Chemicals

The following reagents were used: D-Ala(2)-N-Me-Phe (4)-Glyol(5)-enkephalin (DAMGO), (+)-4-[(aR)-a-((2S,5R)-4-allyl-2,5-dimethyl-1-piperazinyl)-3-methoxybenzyl]-N,N-diethylbenzamide (SNC80), (−)-trans3,4-dichloro-N-methyl-N[2(pyrrolidinyl)-cyclohexyl]-benzeneacetamide (U-50488H), forskolin, 3-isobutyl-1-methylxanthine (IBMX), Ro 20-1724 (Sigma-Aldrich), Halo-Tag pH Sensor Ligand (Promega Corp), Hoechst 33342 (Dojinkagaku), morphine hydrochloride (Takeda Pharmaceutical Co, Ltd), and fentanyl (Janssen Pharmaceutical K.K.). N1, N2, forskolin, IBMX, and Ro 20-1724 were diluted with dimethyl sulfoxide (DMSO), while other reagents were diluted with H_2O.

Functional Analysis of ORs With the CellKey System

The CellKey assay system has been described previously.[24] Briefly, cells stably expressing Halotag MOR/pGS22F, Halotag DOR/pGS22F, or Halotag KOR/pGS22F were seeded at densities of 6.0×10^4 (Halotag MOR/pGS22F) or 5.0×10^4 (Halotag DOR/pGS22F and Halotag KOR/pGS22F) in poly-D-Lysine (Sigma Aldrich)-coated CellKey 96-well microplates and incubated for 24 hours. The wells were washed with a CellKey buffer composed of Hank's balanced salt solution (in mM: 1.3 $CaCl_2 \cdot 2H_2O$, 0.81 $MgSO_4$, 5.4 KCl, 0.44 KH_2PO_4, 4.2 $NaHCO_3$, 136.9 NaCl, 0.34 Na_2HPO_4, and 5.6 D-glucose) containing 20 mM 4-(2-hydroxyethyl)-1-piperazineethanesulfonic acid (HEPES) and 0.1% BSA. Cells were incubated for 30 minutes at 28 °C before the assay, in accordance with the protocol described by Manabe et al.[17] Changes in the impedance current (ΔZiec) in each well were measured at 10-second intervals for up to 30 minutes while considering the first 5 minutes as baseline, and ΔZiec measurements were obtained for 25 minutes after administration of each compound. The ΔZiec values for each sample were corrected using the values of the negative control sample (mean of data of duplicate wells in cells treated with vehicle). The positive controls in ΔZiec measurements were DAMGO for Halotag MOR/pGS22F, SNC80 for Halotag DOR/pGS22F, and U-50488H for Halotag KOR/pGS22F. These data were plotted the average value of the date obtained in the 3 experiments for each concentration and created a concentration-response curve, using GraphPad Prism 8. Each drug was measured in duplicate (1 drug, 1 concentration/2 wells) in a 96-well microplate. In this study, we set n = 1/well. The average value of the date obtained in the 3 experiments was plotted for each concentration, and a concentration-response curve was created using GraphPad Prism8. Statistical analysis was performed using the nonlinear regression three parameter.

Intracellular cAMP Assay With GloSensor

The GloSensor cAMP assay was performed as described by Manabe et al[17] and Meguro et al.[25] Briefly, cAMP accumulation was analyzed using cells stably expressing Halotag MOR/pGS22F, Halotag DOR/pGS22F, or Halotag KOR/pGS22F. The cells were seeded at 4.0×10^4 cells/well in 96-well clear-bottom plates (Corning Inc) and then incubated for 24 hours. After washing the cells with CellKey buffer without BSA, the cells were equilibrated with diluted GloSensor reagent at room temperature for 2 hours, and the baseline luminescence intensity was measured for 15 minutes. After the baseline measurement, cells were treated with the test compounds for 10 minutes, and forskolin (3.0×10^{-6} M) was then added.[17,25] The luminescence intensity was measured every 2.5 minutes for 30 minutes using Synergy H1 (BioTek Instruments Inc), time-luminescence curves were traced, and the area under the curve (AUC) values

of time-luminescence intensity were calculated. The responses for each compound were expressed as the AUC of each compound subtracted from that of the negative control sample (mean of data of duplicate wells in cells treated with forskolin alone). Data are presented as the percentage of intracellular cAMP inhibition calculated by dividing the corrected AUC by those of the standard sample (mean of data of duplicate wells in cells treated with positive control). The standard samples were DAMGO (10^{-5} M) for Halotag MOR/pGS22F, SNC80 (10^{-5} M) for Halotag DOR/pGS22F, and U-50488H (10^{-7} M) for Halotag KOR/pGS22F. These data were plotted with average values obtained in 3 experiments for each concentration, and concentration-response curves were created using GraphPad Prism 8. Each drug was measured in duplicate (1 drug, 1 concentration/2 wells) in a 96-well microplate. In this study, we set n = 1/well. The average value of the date obtained in the 3 experiments was plotted for each concentration, and a concentration-response curve was created using GraphPad Prism8. Statistical analysis was performed using the nonlinear regression three parameter.

β-Arrestin Recruitment Assay With PathHunter

The β-arrestin recruitment assay was performed according to the protocol for PathHunter (DiscoverX). U2OS OPRM1, CHO-K1 OPRD1, or U2OS OPRK1 cells were seeded at a density of 1.0×10^4 cells/well in 96-well clear-bottom white plates and incubated for 48 hours. The cells were stimulated for 90 minutes (MOR and DOR) or 180 minutes (KOR) with a dilution series of each receptor at 37 °C and 5% CO_2, and PathHunter working detection solution was added. Luminescence intensity was measured using FlexStation 3 (BioTek Instruments Inc) for 1 hour at room temperature. Data are expressed as percentage of positive control (maximum signal intensity of each test compound/that of positive control). These data were plotted the average value of the date obtained in the 3 experiments for each concentration and created a concentration-response curve, using GraphPad Prism 8. Each drug was measured in duplicate (1 drug, 1 concentration/2 wells) in a 96-well microplate. In this study, we set n = 1/well. The average value of the date obtained in the three experiments was plotted for each concentration, and a concentration-response curve was created using GraphPad Prism8. Statistical analysis was performed using the nonlinear regression three parameter.

Internalization Assay of ORs

The internalization assay for each OR was performed according to the protocol described by Manabe et al.[17] Briefly, cells stably expressing Halotag MOR/pGS22F (1.2×10^5), Halotag DOR/pGS22F, or Halotag KOR/pGS22F (1.05×10^5) were seeded in a polyethylenimine-coated 8-well chamber slide system. After incubation for 24 hours, cells were stained with Hoechst 33342 for 10 minutes followed by the pH sensor ligand (0.5×10^{-6} M) for 15 minutes (incubated in 5% CO_2 at 37 °C) and washed once with the internalization buffer (10 mM HEPES, 140 mM NaCl, 5 mM KCl, 2 mM $CaCl_2$, 1 mM $MgCl_2$, and 10 D-glucose at pH 7.4). Red spots in the cells were recorded every 10 minutes after compound treatment for 120 minutes using TCS SP8 LIGHTNING (Leica Microsystems). Each Image was observed at 16-bit gray scale. The numbers of both red spots and nuclei were counted using MetaMorph 7.7 (Molecular Devices). Data were quantified as "Gray value/cell."

Animal Studies

Six- to 12-week-old C57BL/6JJmsSlc mice (Japan SLC) were used in this study. Mice were maintained under standard laboratory conditions (temperature: 23 °C ± 3 °C, relative humidity: 55% ± 15%, 12-hour light/dark cycle [lighting from 600 to 1800 hours]), with free access to commercial meals (CRF-1; Oriental Yeast Co, Ltd) and water. Animals were randomly assigned to each group based on their pain response and body weight. During the experiments, efforts were made to minimize the suffering of the animals as well as the number of animals used.

Mouse Tail-Flick Test

Analgesic evaluation was performed using the tail-flick unit (Ugo Basile). In the tail-flick test, a thermal stimulus was applied to the tail of mice, and the latency(s) of the tail withdrawal reflex was measured according to the method described by D'Amour and Smith.[26] The maximum irradiation (cutoff) time was 10 seconds to prevent burns. The test substance was subcutaneously administered (10 mL/kg) to the mice, and tail withdrawal latency at each time point (up to 90 minutes) after the administration was measured.

Fentanyl-Tolerant Mouse Model

Fentanyl-tolerant mouse models were obtained by repetitive subcutaneous administration of fentanyl (0.03 mg/kg) to mice 3 times a day for 3 days. On the fourth day, test compounds (fentanyl [0.03 mg/kg], morphine, N1 [3 mg/kg], or N2 [10 mg/kg]) were subcutaneously administered, and the analgesic effect was evaluated using the tail-flick test.

Statistical Analysis

The sample size for each experiment was determined based on effect size calculated from the standard deviation of preliminary data, a power of 0.8, and significance level of 0.05. Data analyses and concentration-response curve fitting were performed using GraphPad Prism 8 (GraphPad Software).

Data are presented as means with standard error of the mean (SEM) for at least 3 independent experiments. Statistical analysis was performed using the Mann-Whitney test or 2-way analysis of variance (ANOVA) followed by the Tukey-Kramer test (GraphPad Prism 8). $P < .05$ was considered statistically significant. The ED_{50} in the tail-flick test for each compound was calculated using the profit analysis. In the tail-flick test, the ED_{50} was defined as the dose calculated as the 50% activity value when the latency(s) immediately before drug administration (pre) was 0% and the E_{max} (latency = 10 s) was 100%. The Wilcoxon rank-sum test was used for statistical analysis in the fentanyl continuous throw model. The SAS System (SAS Software Release 9.1.3, SAS Institute Japan Ltd) was used in statistical calculations for the tail-flick test.

RESULTS

Evaluation of Transdermal Permeation Rates of N1 and N2

We synthesized 2 novel opioid compounds, N1 and N2 (Figure 1A). To assess the permeation properties of N1 and N2, we measured their transdermal permeation rates using hairless mouse skin. Tulobuterol, in a transdermal preparation used clinically, was used as the positive control.[23] The transdermal absorption rates of N1 and N2 were 1.71 ± 0.35 and 3.94 ± 1.36 $\mu g \cdot cm^{-2} \cdot h^{-1}$, respectively, and that of tulobuterol was 4.42 ± 0.42 $\mu g \cdot cm^{-2} \cdot h^{-1}$.

Effects of N1 and N2 on the Functions of ORs With the CellKey System

We examined the effects of N1 and N2 on 3 types of ORs by using the CellKey system in HEK293 cells expressing either Halotag MOR/pGS22F, Halotag DOR/pGS22F, or Halotag KOR/pGS22F. The CellKey system can detect the activities of GPCRs, including ORs, as changes in cellular impedance.[24] We compared the changes in impedance induced by N1, N2, fentanyl, and morphine with the positive controls for MOR (DAMGO), DOR (SNC80), and KOR (U-50488H). All profiles were obtained for all test compounds (Figure 1B–D; Table 1). The specific E_{max} values for MOR, DOR, and KOR of fentanyl, morphine, N1, and N2 are shown in the Table. Fentanyl, morphine, N1, and N2 all showed the highest efficacy with MOR among the 3 ORs examined, and all acted as full MOR agonists (Figure 1B; Table 1). Considering the E_{max} values, N2 showed significantly higher efficacy than morphine for DOR (Figure 1C, D; Table 1). The EC_{50} values for MOR were in the following order: fentanyl < morphine < N2 ≦ N1 (Table). On the other hand, N1 and N2 elicited partial agonist activity for DOR and KOR (Figure 1C, D).

Effects of N1 and N2 on Intracellular cAMP Levels Measured With the GloSensor cAMP Assay

We measured the intracellular cAMP levels for each OR as an indicator of the G protein–mediated pathway using HEK293 cells expressing Halotag MOR/pGS22F, Halotag DOR/pGS22F, or Halotag KOR/pGS22F. We then compared the effects of N1 and N2 to those of fentanyl and morphine. The E_{max} value of these test compounds for MOR was in the following order: morphine ≦ N1 ≦ N2 ≦ fentanyl (Table 1). Fentanyl, morphine, N1, and N2 all showed the highest efficacy and full agonist activity for MOR (Figure 1E; Table 1). N1 and N2 elicited partial agonist activity for DOR and KOR; N1 showed significantly higher efficacy than fentanyl but similar efficacy to morphine for KOR, while N2 showed significantly higher efficacy than both fentanyl and morphine for DOR and lower efficacy than morphine but similar efficacy to fentanyl for KOR. The EC_{50} values for MOR were in the following order: fentanyl < N2 ≦ morphine < N1 (Figure 1F, G; Table 1).

Effects of N1 and N2 on the Functions of β-Arrestin Recruitment With the PathHunter Assay

Additional accurate quantification was performed using the PathHunter β-arrestin recruitment assay in CHO-K1 cells expressing MOR and DOR (DiscoverX) and U2OS cells expressing KOR (DiscoverX). As shown in Figure 2 and Table 2, only fentanyl elicited full agonist activity, whereas morphine, N1, and N2 elicited partial agonist activity for MOR. In addition, N1 and N2 showed significantly lower efficacy than fentanyl and morphine alone (Table 2). For both DOR and KOR, fentanyl, morphine, N1, and N2 elicited partial agonist activity (Figure 2B, C). Among N1 and N2, N1 had significantly higher efficacy than fentanyl for KOR, whereas N2 showed higher efficacy than both morphine and fentanyl for DOR (Figure 2B, C; Table 2).

Visual Internalization Assay of ORs in Cells Stably Expressing Halotag Tagged ORs

We performed an internalization assay of ORs as a β-arrestin–mediated signaling pathway.[17] We used HEK293 cells stably expressing Halotag MOR/pGS22F, Halotag DOR/pGS22F, or Halotag KOR/pGS22F, in which the Halotag was previously stained with the pH sensor ligand to visualize the internalized ORs induced by each compound.[17] The pH sensor Halotag ligand is impermeable to cell membranes so that it binds to Halotag bound receptors on the membranes. The sensor increases red fluorescence as the pH decreases.[17] Since internalized receptors are incorporated into the endoplasmic reticulum at a low pH, only internalized receptors can be visualized as red fluorescence over time.[17] For MOR, the numbers

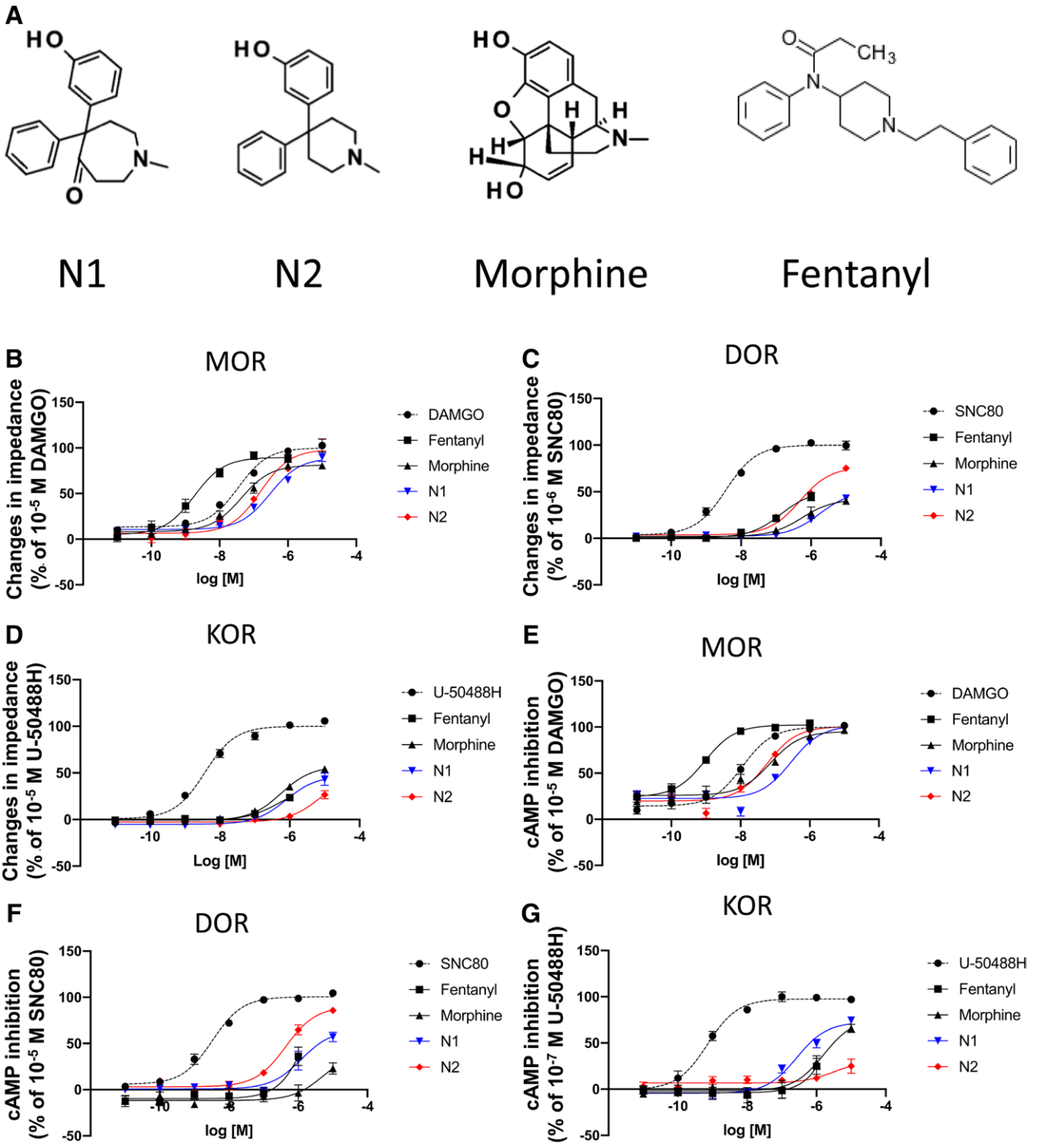

Figure 1. Chemical formula of N1 and N2 and effects of these compounds on ORs in the G protein–mediated pathways. A, Molecular structures of the test compounds. B–G, Effect of each analgesic on MOR, DOR, and KOR activities in the G protein–mediated pathway. Cells expressing MOR (B), DOR (C), and KOR (D) were treated with morphine, fentanyl, N1, and N2 (10^{-11}–10^{-5} M), and changes in impedance (ΔZiec) were measured using the CellKey system. Concentration-response curves were prepared by calculating ΔZiec relative to the data obtained for each positive control: 10^{-5} M DAMGO for MOR (B), 10^{-6} M SNC80 for DOR (C), and 10^{-5} M U-50488H for KOR (D). Cells expressing MOR (E), DOR (F), or KOR (G) were treated with various concentrations (10^{-11}–10^{-5} M) of each compound, and intracellular cAMP levels were measured using the GloSensor cAMP assay. Concentration-response curves were prepared by calculating cAMP levels relative to the data obtained with 10^{-5} M DAMGO for MOR (E), 10^{-5} M SNC80 for DOR (F), and 10^{-7} M U-50488H for KOR (G). In one experiment in this study, each drug was measured in duplicate (1 drug, 1 concentration/2 wells each) in a 96-well microplate. We analyzed with the average value of 2 wells set to n = 1. The data are presented as mean ± SEM for 3 independent experiments (n = 3). cAMP indicates cyclic adenosine monophosphate; DAMGO, D-Ala(2)-N-Me-Phe(4)-Glyol(5)-enkephalin; DOR, δ-opioid receptor; KOR, κ-opioid receptor; MOR, μ-opioid receptor; N1, new opioid 1; N2, new opioid 2; SEM, standard error of the mean; SNC80, (+)-4-[(aR)-a-((2S,5R)-4-allyl-2,5-dimethyl-1-piperazinyl)-3-methoxybenzyl]-N,N-diethylbenzamide; U-50488H, trans3,4-dichloro-N-methyl-N[2(pyrrolidinyl)-cyclohexyl]-benzeneacetamide; ΔZiec, impedance current.

Table 1. $LogEC_{50}$ and E_{max} Values of N1, N2, or Opioid Analgesics With the CellKey and cAMP Assays in ORs

	MOR		DOR		KOR	
CellKey assay	**$LogEC_{50}$ (M)**	**E_{max} (%w)**	**$LogEC_{50}$ (M)**	**E_{max} (%)**	**$LogEC_{50}$ (M)**	**E_{max} (%)**
Fentanyl	−8.74 ± 0.14	89.5 ± 3.70	−6.86 ± 0.13	44.8 ± 4.51	n.d.	33.7 ± 4.99
Morphine	−7.37 ± 0.12	81.3 ± 3.16	−6.26 ± 0.16	40.0 ± 1.76	−6.25 ± 0.07	56.9 ± 1.96
N1	−6.52 ± 0.11[a,b]	89.0 ± 3.92 ns, ns	−5.76 ± 0.07 ns, ns	40.0 ± 1.76 ns, ns	−6.11 ± 0.13 ns	46.7 ± 3.75 ns, ns
N2	−6.80 ± 0.12[a,c]	98.4 ± 4.61 ns	−6.32 ± 0.07 ns, ns	75.2 ± 2.85[d] ns	n.d.	46.3 ± 16.50 ns, ns
cAMP assay						
Fentanyl	−9.03 ± 0.09	102.2 ± 2.23	n.d.	36.1 ± 10.02	n.d.	24.7 ± 8.63
Morphine	−7.15 ± 0.14	95.3 ± 3.89	n.d.	22.9 ± 6.00	−5.79 ± 0.18	65.7 ± 4.31
N1	−6.54 ± 0.14[a,c]	101.4 ± 4.80 ns, ns	−5.96 ± 0.19	57.2 ± 5.17 ns, ns	−6.57 ± 0.12 ns	74.6 ± 2.46[a] ns
N2	−7.24 ± 0.11[a] ns	100.5 ± 3.53 ns, ns	−6.36 ± 0.10	85.7 ± 2.04[a,b]	n.d.	24.9 ± 7.6 ns

E_{max} (means ± SEM) and $LogEC_{50}$ were calculated according to the results in Figures 1 and 2.
P values in $LogEC_{50}$ of MOR in CellKey assay: fentanyl versus morphine, $P < .0001$; fentanyl versus N1, $P < .0001$; fentanyl versus N2, $P < .0001$; morphine versus N1, $P = .0002$; morphine versus N2, $P = .0386$.
P values in E_{max} of MOR in CellKey assay: fentanyl versus morphine, $P = .8126$; fentanyl versus N1, $P > .9999$; fentanyl versus N2, $P = .7734$; morphine versus N1, $P = .8561$; morphine versus N2, $P = .0716$.
P values in $LogEC_{50}$ of DOR in CellKey assay: fentanyl versus morphine, $P = .9996$; fentanyl versus N1, $P = .9642$; fentanyl versus N2, $P = .9998$; morphine versus N1, $P > .9999$; morphine versus N2, $P > .9999$.
P values in E_{max} of DOR in CellKey assay: fentanyl versus morphine, $P = .9976$; fentanyl versus N1, $P > .9999$; fentanyl versus N2, $P = .3067$; morphine versus N1, $P = .9984$; morphine versus N2, $P = .0459$.
P values in $LogEC_{50}$ of KOR in CellKey assay: morphine versus N1, $P > .9999$.
P values in E_{max} of KOR in CellKey assay: fentanyl versus morphine, $P = .1816$; fentanyl versus N1, $P = .8725$; fentanyl versus N2, $P = .8913$; morphine versus N1, $P > .9704$; morphine versus N2, $P > .9999$.
P values in $LogEC_{50}$ of MOR in cAMP assay: fentanyl versus morphine, $P = .0007$; fentanyl versus N1, $P < .0001$; fentanyl versus N2, $P = .0041$; morphine versus N1, $P = .0236$; morphine versus N2, $P > .9999$.
P values in E_{max} of MOR in cAMP assay: fentanyl versus morphine, $P = .8126$; fentanyl versus N1, $P > .9999$; fentanyl versus N2, $P = .7734$; morphine versus N1, $P = .8561$; morphine versus N2, $P = .0716$.
P values in E_{max} of DOR in cAMP assay: fentanyl versus morphine, $P > .9999$; fentanyl versus N1, $P = .3699$; fentanyl versus N2, $P = .0013$; morphine versus N1, $P = .6252$; morphine versus N2, $P = .0048$.
P values in $LogEC_{50}$ of KOR in cAMP assay: morphine versus N1, $P = .05384$.
P values in E_{max} of KOR in cAMP assay: fentanyl versus morphine, $P < .0001$; fentanyl versus N1, $P < .0001$; fentanyl versus N2, $P > .9999$; morphine versus N1, $P = .9704$; morphine versus N2, $P < .0001$.
Abbreviations: cAMP, cyclic adenosine monophosphate; DOR, δ-opioid receptor; KOR, κ-opioid receptor; MOR, μ-opioid receptor; N1, new opioid 1; N2, new opioid 2; n.d., not detected; ns, not significant; OR, opioid receptor; SEM, standard error of mean.
[a]$P < .01$ versus fentanyl.
[b]$P < .01$ versus morphine.
[c]$P < .05$ versus fentanyl.
[d]$P < .05$ versus morphine.

Table 2. $LogEC_{50}$ and E_{max} Values of N1, N2, or Opioid Analgesics With the β-Arrestin Assay in ORs

	MOR		DOR		KOR	
β-arrestin assay	**$LogEC_{50}$ (M)**	**E_{max} (%)**	**$LogEC_{50}$ (M)**	**E_{max} (%)**	**$LogEC_{50}$ (M)**	**E_{max} (%)**
Fentanyl	−7.16 ± 0.08	72.15 ± 3.20	n.d.	2.45 ± 0.97	−7.58 ± 0.63	1.63 ± 1.32
Morphine	−5.68 ± 0.03[a]	32.63 ± 0.70[a]	n.d.	5.32 ± 0.49	n.d.	12.59 ± 1.46
N1	−5.47 ± 0.32[a], ns	19.46 ± 4.54[a,b]	−5.65 ± 0.77	2.84 ± 0.87 ns, ns	−5.17 ± 0.46[c]	14.93 ± 2.02[a], ns
N2	−5.77 ± 0.07[a], ns	19.34 ± 0.86[a,b]	−6.06 ± 0.11	10.79 ± 0.80[a,d]	−7.71 ± 0.91 ns	0.70 ± 2.00[d], ns

E_{max} (means ± SEM) and $LogEC_{50}$ were calculated according to the results of Figure 3.
P values in $LogEC_{50}$ of MOR: fentanyl versus morphine, $P = .0014$; fentanyl versus N1, $P = .0001$; fentanyl versus N2, $P = .0010$; morphine versus N1, $P = .8840$; morphine versus N2, $P = .9917$.
P values in E_{max} of MOR: fentanyl versus morphine, $P < .0001$; fentanyl versus N1, $P < .0001$; fentanyl versus N2, $P < .0001$; morphine versus N1, $P = .0426$; morphine versus N2, $P = .0405$.
P values in E_{max} of DOR: fentanyl versus morphine, $P = .0880$; fentanyl versus N1, $P > .9858$; fentanyl versus N2, $P < .0001$; morphine versus N1, $P = .1651$; morphine versus N2, $P = .0006$.
P values in $LogEC_{50}$ of KOR: fentanyl versus N1, $P = .0461$; fentanyl versus N2, $P = .9901$.
P values in E_{max} of KOR: fentanyl versus morphine, $P = .0012$; fentanyl versus N1, $P = .0001$; fentanyl versus N2, $P = .9806$; morphine versus N1, $P = .7746$; morphine versus N2, $P = .0005$.
Abbreviations: DOR, δ-opioid receptor; KOR, κ-opioid receptor; MOR, μ-opioid receptor; N1, new opioid 1; N2, new opioid 2; n.d., not detected; ns, not significant; OR, opioid receptor; SEM, standard error of mean.
[a]$P < .01$ versus fentanyl.
[b]$P < .05$ versus morphine.
[c]$P < .05$ versus fentanyl.
[d]$P < .01$ versus morphine.

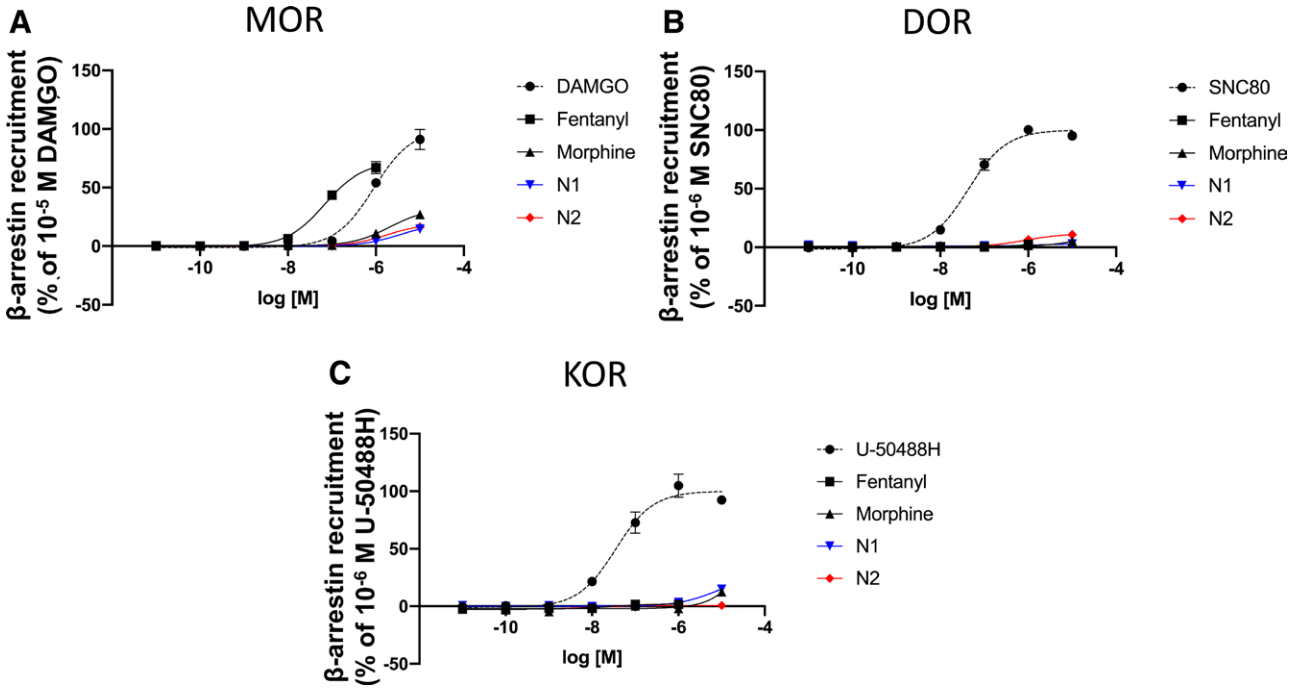

Figure 2. Levels of β-arrestin recruitment in ORs induced by N1, N2, or opioid analgesics. The β-arrestin assay was performed in cells expressing MOR (A), DOR (B), and KOR (C) and treated with each of the compounds (10^{-11}–10^{-5} M). Concentration-response curves were prepared by calculating intracellular β-arrestin levels relative to the data obtained for each positive control: 10^{-5} M DAMGO for MOR (A), 10^{-6} M SNC80 for DOR (B), and 10^{-6} M of U-50488H for KOR (C). In one experiment in this study, each drug was measured in duplicate (1 drug, 1 concentration/2 wells each) in a 96-well microplate. We analyzed with the average value of 2 wells set to n = 1. All points are presented as mean ± SEM for 3 independent experiments (n = 3). DAMGO indicates D-Ala(2)-N-Me-Phe(4)-Glyol(5)-enkephalin; DOR, δ-opioid receptor; KOR, κ-opioid receptor; MOR, μ-opioid receptor; N1, new opioid 1; N2, new opioid 2; OR, opioid receptor; SEM, standard error of the mean; SNC80, (+)-4-[(aR)-a-((2S,5R)-4-allyl-2,5-dimethyl-1-piperazinyl)-3-methoxybenzyl]-N,N-diethylbenzamide; U-50488H, trans3,4-dichloro-N-methyl-N[2(pyrrolidinyl)-cyclohexyl]-benzeneacetamide.

and intensity of red spots were increased by fentanyl and DAMGO over time (Figure 3A). Morphine, N1, and N2 showed time-dependent but slight accumulation of red spots in cells; however, the values were not statistically significant (Figure 3A).

For DOR and KOR, the number and intensity of red spots increased over time only with SNC80 and U-50488H, respectively (Figure 3B, C). Fentanyl, morphine, N1, and N2 did not show significant differences from the vehicle (Figure 3B, C).

Mouse Tail-Flick Test

We evaluated the analgesic efficacy of N1 and N2 by using the tail-flick analgesic efficacy test and then compared the findings with those for fentanyl and morphine. First, we analyzed the analgesic actions using several concentrations of each opioid. The ED_{50} values for fentanyl, morphine, N1, and N2 were 0.019, 2.3, 1.6, and 5.3 mg/kg, respectively (Supplemental Digital Content 1, Table 1, http://links.lww.com/AA/D877). Based on the ED_{50} value of each opioid (Supplemental Digital Content 1, Table 1, http://links.lww.com/AA/D877), we determined the doses for evaluation of analgesic efficacy as follows: fentanyl, 0.03 mg/kg; morphine and N1, 3 mg/kg; and N2, 10 mg/kg. As shown in Figure 4A, N1 and N2 showed the same levels of analgesic efficacy as morphine (Figure 4A; Supplemental Digital Content 1, Table 1, http://links.lww.com/AA/D877).

We then subcutaneously administered fentanyl 3 times a day for 3 to create fentanyl-tolerant model mice, and we evaluated the analgesic effects of the test compounds on day 4. In the model mice induced by repetitive fentanyl administration, fentanyl injected on the fourth day showed a significantly diminished analgesic action (Figure 4B). On the other hand, no diminution in the analgesic effect was observed after morphine injection into the fentanyl-tolerant mice (Figure 4C). Furthermore, in the model mice, neither N1 nor N2 showed diminished analgesic effects (Figure 4D, E).

DISCUSSION

Patch preparations are widely used in various clinical treatments because they do not require administration devices, are convenient, and provide more certain and stable blood concentrations than oral preparations.[4,5,8,9,27,28] However, in analgesic treatment, the fentanyl patch is the only potent opioid patch currently available. Fentanyl patches are often used because of the transdermal activity of fentanyl, but they often result in tolerance, in some cases necessitating a change to other opioids.[10–12]

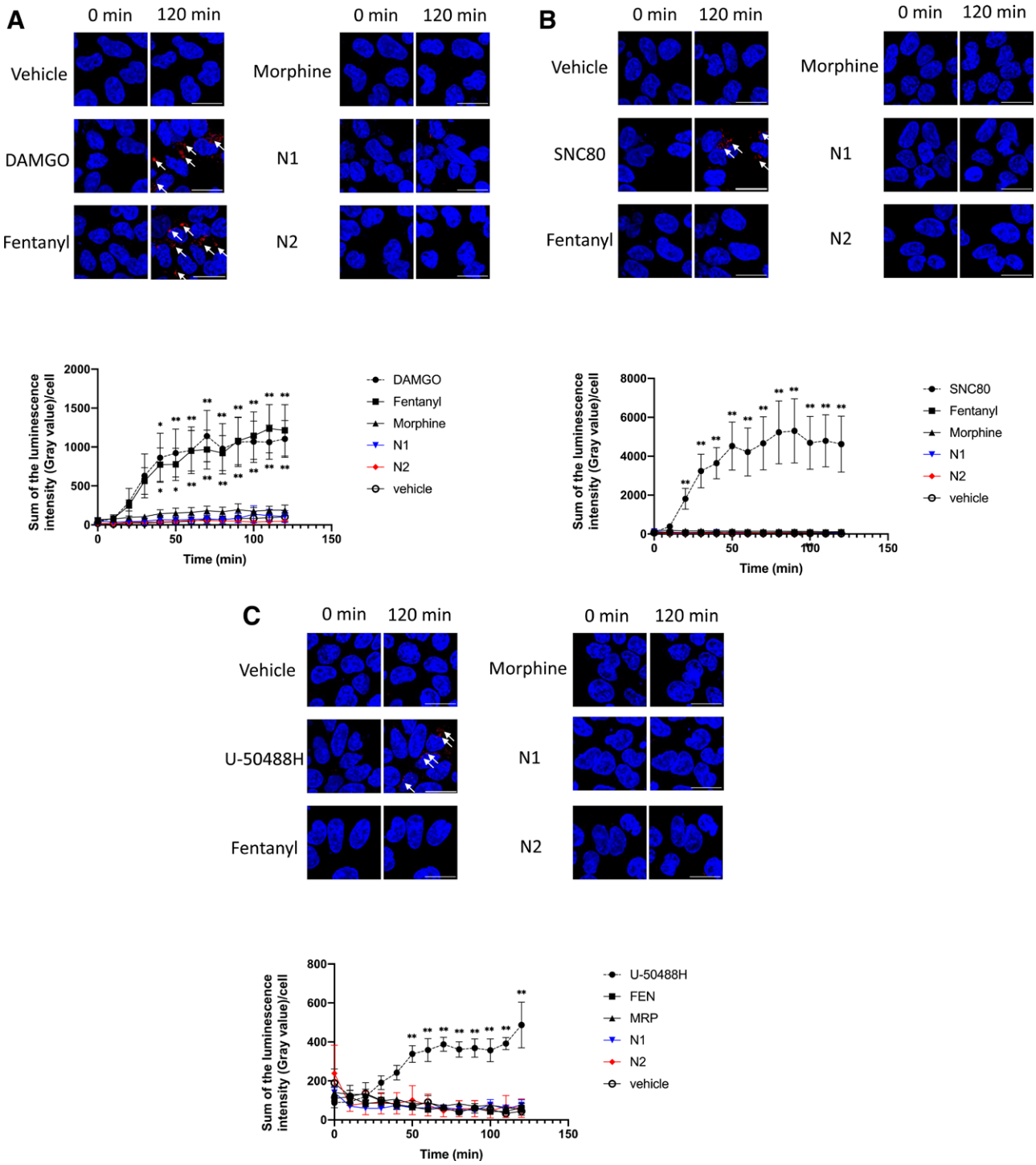

Figure 3. Internalization of ORs induced by N1, N2, or opioid analgesics in HEK293 cells stably expressing Halotag ORs. HEK293 cells stably expressing Halotag MOR (A), DOR (B), or KOR (C) were stained with Hoechst 33342 (blue) and the Halotag pH sensor ligand (red); treated with each compound or vehicle for up to 120 min; and observed at the indicated time points. To quantify internalization levels, the numbers and intensities of red spots and nuclei were counted using MetaMorph 7.7. The data were quantified by "sum of intensity/cell" and normalized by the values obtained before compound application (% of sum of intensity/cell before compound application). All data are presented as mean ± SEM (n = 3–5). $*P < .05$ and $**P < .01$, versus vehicle. DAMGO indicates D-Ala(2)-N-Me-Phe(4)-Glyol(5)-enkephalin; DOR, δ-opioid receptor; HEK293, human embryonic kidney 293; KOR, κ-opioid receptor; MOR, μ-opioid receptor; N1, new opioid 1; N2, new opioid 2; OR, opioid receptor; SEM, standard error of the mean.

The newly synthesized N1 and N2 had better transpermeability to the skin permeability than morphine. Our in vitro and in vivo experiments showed that N1 and N2 had analgesic effects similar to that of morphine. The transdermal absorption rates of N1 and N2 were superior to those of fentanyl and

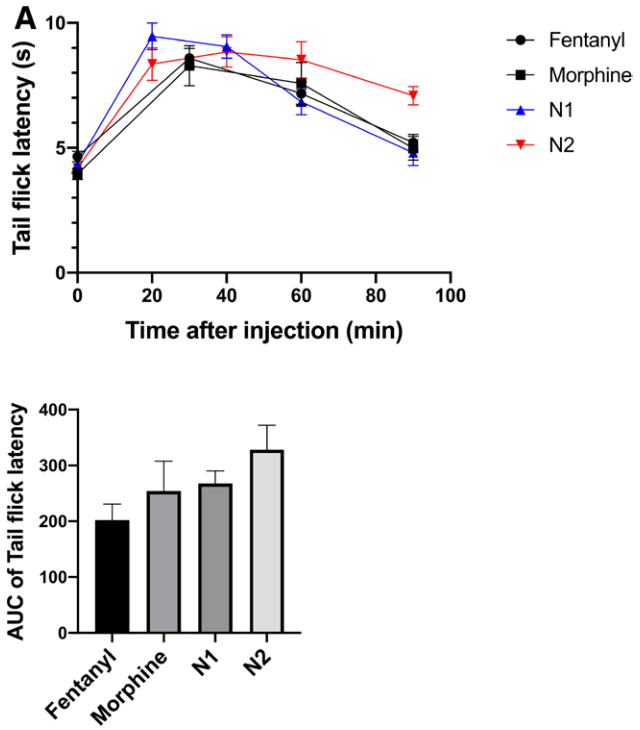

Figure 4. Analgesic actions of N1, N2, and opioid analgesics in the tail-flick test. Mice were administered fentanyl (0.03 mg/kg, n = 7), morphine (3 mg/kg; n = 8), N1 (3 mg/kg; n = 8), or N2 (10 mg/kg; n = 8). After administration, analgesic effects were measured using the tail-flick test (A). Effects of fentanyl (B) (0.03 mg/kg, control; n = 8, fentanyl-tolerant mice; n = 8), morphine (C) (3 mg/kg, control; n = 8, fentanyl-tolerant mice; n = 7), N1 (D) (3 mg/kg, control; n = 7, fentanyl-tolerant mice; n = 7), and N2 (E) (10 mg/kg, control; n = 7, fentanyl-tolerant mice; n = 7) on the fentanyl-tolerant mice. Figures on the left indicated a time course of tail-flick latency, and those on the right showed the AUC of a time course of tail-flick latency of each mouse. All data are presented as mean ± SEM (n = 7–8). **P* < .05 and ***P* < .01, versus vehicle preadministration. AUC indicates area under the curve; N1, new opioid 1; N2, new opioid 2; SEM, standard error of the mean.

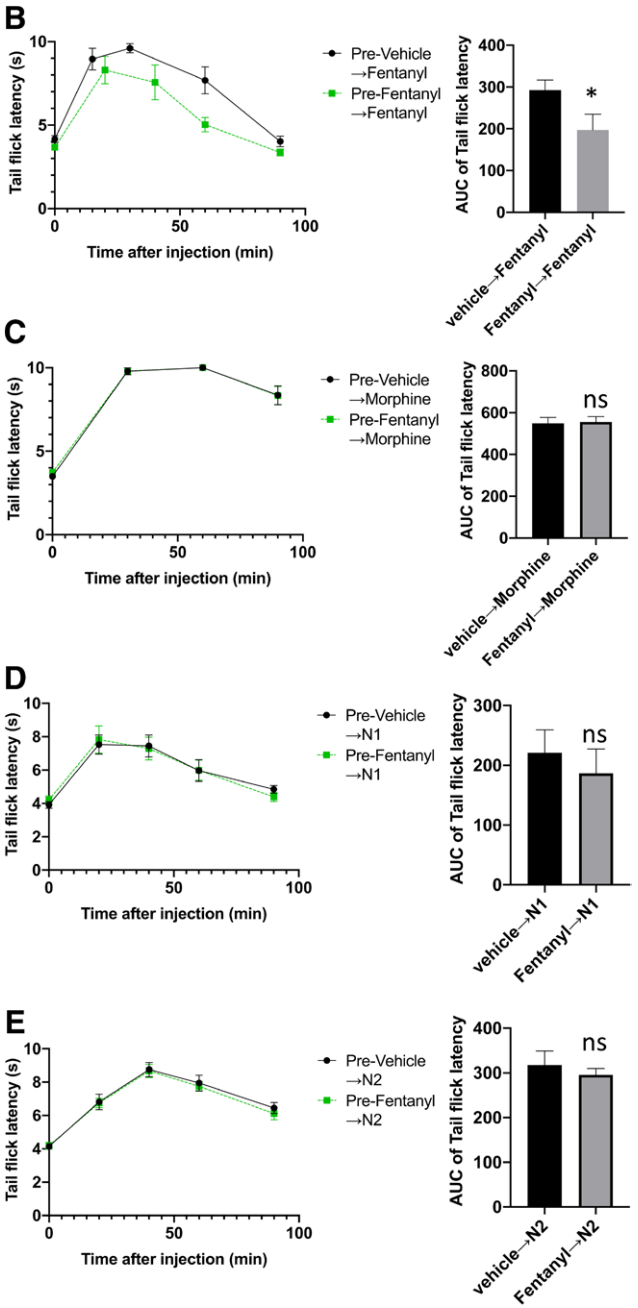

Figure 4. Continued.

morphine reported in a prior study.[6] In the transdermal absorption study, the difference in the absorption of compounds is well correlated in the vitro and vivo experiments.[29] Tulobuterol was used as a comparative object in this experiment, since tulobuterol is a typical patch preparation widely used in clinical practice. These results suggest that N1 and N2 are transdermally absorbable compounds and may be candidates for analgesic patch development.

The activation of ORs elicits 2 downstream pathways; one leads to mainly analgesic effects through G protein–mediated pathways and the other causes analgesic opioid tolerance through β-arrestin–mediated pathways.[17,30] We evaluated these pathways using CellKey and the cAMP assay to measure whole-cell activity and only G protein–mediated pathways, respectively. In our previous study, the results with the CellKey system seemed to be mainly G protein-mediated.[17,24] In the present study, N1 and N2 showed the highest efficacy for MOR in both assays, which was similar to the findings for fentanyl and morphine. These results suggest that both N1 and N2 are full agonists of MOR. The EC_{50} values measured by the CellKey assay were in the order of fentanyl < morphine < N2 ≦ N1, while those measured by the cAMP assay were in the order of fentanyl < N2 ≦ morphine < N1. On the basis of these results, N2 may have superior potency for G protein–dependent signals than N1, although the detailed mechanism in relation to their structural differences remains obscure.

In several studies with β-arrestin-2 knockout mice, enhanced and prolonged analgesic effects of

morphine were reported.[30,31] In addition, resistance to morphine was also reduced in this model; respiratory depression was suppressed, and resistance to colon function was not observed.[30–33] In our β-arrestin recruitment assay with MOR, only fentanyl acted as a full agonist, whereas morphine, N1, and N2 were partial agonists. Both N1 and N2 showed significantly lower efficacy than fentanyl and morphine in β-arrestin–dependent activities. Our internalization assay with MOR showed that N1 and N2 have lower β-arrestin–mediated pathway-activating profiles than fentanyl, similar to morphine. Taken together, these data indicate that N1 and N2 are biased G protein–dependent pathway agonists, suggesting that they might have analgesic actions with fewer deleterious opioid effects, including tolerance, although further in vivo studies are needed.

In the study with DOR, N2 showed the maximal activation profile among the opioids examined. DOR agonists show fewer potent analgesic effects than MOR agonists,[34,35] but they cause less sedation, respiratory depression, and gastrointestinal motility suppression than MOR agonists; thus, they may be candidates for novel analgesics with fewer side effects.[34,35] In fact, to achieve effective analgesia, multiple sites of action must be targeted.[35] Some studies have shown that access to both the brainstem and spinal cord by DOR agonists provides synergistic analgesia and yields a dose-response curve shifted to the left relative to the curve for the lone targeting of either structure.[35] In addition, some reports have shown that DOR agonists can attenuate allodynia and hyperalgesia in a rat model of neuropathic pain[36]; they have also been shown to have analgesic activity in bone cancer-induced pain models.[35,37] Furthermore, recent reports have shown that DOR agonists have analgesic, antidepressant, anxiolytic, and antimigraine effects, making them attractive therapeutics for such symptoms.[30] N2 might thus be an effective compound with transdermal permeability.

In our animal experiments, N1 and N2 showed analgesic effects equivalent to those of fentanyl and morphine. In the fentanyl tolerance model, sufficient analgesic effects were not achieved with fentanyl; however, N1 and N2 showed almost full analgesic effects, equal to those of morphine. These results suggest that opioid transition is possible in patients with fentanyl resistance by using compounds with N1- or N2-like properties. However, further studies are needed to elucidate the analgesic efficacy of transdermal administration of N1 and N2 in more detail.

In conclusion, we demonstrated that transdermal N1 and N2 show biased G protein–mediated analgesic properties over β-arrestin–mediated pathways, suggesting that N1 and N2 could be analgesics with reduced analgesic tolerance. We believe that these 2 compounds may serve as a foundation for the development of novel transdermal opioids, with compounds that can be used to transition from fentanyl patches safely and effectively. ■

DISCLOSURES

Name: Akane Komatsu, MD.
Contribution: This author helped design this trial, acquire and interpret the data, and draft and revise the manuscript.
Conflicts of Interest: None.
Name: Kanako Miyano, PhD.
Contribution: This author helped design this trial, acquire and interpret the data, and draft and revise the manuscript.
Conflicts of Interest: None.
Name: Daisuke Nakayama, PhD.
Contribution: This author helped design this trial, acquire and interpret the data, and draft and revise the manuscript.
Conflicts of Interest: D. Nakayama is an employee of Daiichi Sankyo Co, Ltd.
Name: Yusuke Mizobuchi, MD.
Contribution: This author helped acquire and interpret the data and revise the manuscript.
Conflicts of Interest: None.
Name: Eiko Uezono, MD.
Contribution: This author helped acquire and interpret the data and revise the manuscript.
Conflicts of Interest: None.
Name: Kaori Ohshima, MS.
Contribution: This author helped acquire and interpret the data and revise the manuscript.
Conflicts of Interest: None.
Name: Yusuke Karasawa, MS.
Contribution: This author helped acquire and interpret the data and revise the manuscript.
Conflicts of Interest: None.
Name: Yui Kuroda, MD.
Contribution: This author helped acquire and interpret the data and revise the manuscript.
Conflicts of Interest: None.
Name: Miki Nonaka, PhD.
Contribution: This author helped acquire and interpret the data and revise the manuscript.
Conflicts of Interest: None.
Name: Keisuke Yamaguchi, MD, PhD.
Contribution: This author helped acquire and interpret the data, and revise the manuscript.
Conflicts of Interest: None.
Name: Masako Iseki, MD, PhD.
Contribution: This author helped acquire and interpret the data and revise the manuscript.
Conflicts of Interest: None.
Name: Yasuhito Uezono, MD, PhD.
Contribution: This author helped design this trial, acquire and interpret the data, and draft and revise the manuscript.
Conflicts of Interest: Y. Uezono received grant support from Daiichi Sankyo Co, Ltd.
Name: Masakazu Hayashida, MD, PhD.
Contribution: This author helped acquire and interpret the data and revise the manuscript.
Conflicts of Interest: None.
This manuscript was handled by: Jianren Mao, MD, PhD.

REFERENCES

1. Rodriguez C, Ji M, Wang HL, Padhya T, McMillan SC. Cancer pain and quality of life. *J Hosp Palliat Nurs.* 2019;21:116–123.

2. Blake A, Wan BA, Malek L, et al. A selective review of medical cannabis in cancer pain management. *Ann Palliat Med.* 2017;6:S215–S222.
3. Wiffen PJ, Wee B, Derry S, Bell RF, Moore RA. Opioids for cancer pain—an overview of Cochrane reviews. *Cochrane Database Syst Rev*. 2017;7:Cd012592.
4. Ahn JS, Lin J, Ogawa S, et al. Transdermal buprenorphine and fentanyl patches in cancer pain: a network systematic review. *J Pain Res.* 2017;10:1963–1972.
5. Vithlani RH, Baranidharan G. Transdermal opioids for cancer pain management. *Rev Pain.* 2010;4:8–13.
6. Lehmann KA, Zech D. Transdermal fentanyl: clinical pharmacology. *J Pain Symptom Manage.* 1992;7:S8–16.
7. WHO Guidelines Approved by the Guidelines Review Committee. *WHO Guidelines for the Pharmacological and Radiotherapeutic Management of Cancer Pain in Adults and Adolescents*. World Health Organization © World Health Organization 2018. 2018.
8. Marwah H, Garg T, Goyal AK, Rath G. Permeation enhancer strategies in transdermal drug delivery. *Drug Deliv.* 2016;23:564–578.
9. Kress HG, Von der Laage D, Hoerauf KH, et al. A randomized, open, parallel group, multicenter trial to investigate analgesic efficacy and safety of a new transdermal fentanyl patch compared to standard opioid treatment in cancer pain. *J Pain Symptom Manage.* 2008;36:268–279.
10. Aurilio C, Pace MC, Pota V, et al. Opioids switching with transdermal systems in chronic cancer pain. *J Exp Clin Cancer Res.* 2009;28:61.
11. Mercadante S, Villari P, Ferrera P, Casuccio A. Addition of a second opioid may improve opioid response in cancer pain: preliminary data. *Support Care Cancer.* 2004;12:762–766.
12. Hair PI, Keating GM, McKeage K. Transdermal matrix fentanyl membrane patch (matrifen): in severe cancer-related chronic pain. *Drugs.* 2008;68:2001–2009.
13. Clemens KE, Klaschik E. Clinical experience with transdermal and orally administered opioids in palliative care patients–a retrospective study. *Jpn J Clin Oncol.* 2007;37:302–309.
14. Schmid CL, Kennedy NM, Ross NC, et al. Bias factor and therapeutic window correlate to predict safer opioid analgesics. *Cell.* 2017;171:1165–1175.e13.
15. Raehal KM, Schmid CL, Groer CE, Bohn LM. Functional selectivity at the μ-opioid receptor: implications for understanding opioid analgesia and tolerance. *Pharmacol Rev.* 2011;63:1001–1019.
16. Rovira X, Pin JP, Giraldo J. The asymmetric/symmetric activation of GPCR dimers as a possible mechanistic rationale for multiple signalling pathways. *Trends Pharmacol Sci.* 2010;31:15–21.
17. Manabe S, Miyano K, Fujii Y, et al. Possible biased analgesic of hydromorphone through the G protein-over β-arrestin-mediated pathway: cAMP, CellKey™, and receptor internalization analyses. *J Pharmacol Sci.* 2019;140:171–177.
18. Okude J, Ueda T, Kofuku Y, et al. Identification of a conformational equilibrium that determines the efficacy and functional selectivity of the μ-Opioid receptor. *Angew Chem Int Ed Engl.* 2015;54:15771–15776.
19. Raffa RB, Martinez RP, Connelly CD. G-protein antisense oligodeoxyribonucleotides and mu-opioid supraspinal antinociception. *Eur J Pharmacol.* 1994;258:R5–R7.
20. Bohn LM, Lefkowitz RJ, Gainetdinov RR, Peppel K, Caron MG, Lin FT. Enhanced morphine analgesia in mice lacking beta-arrestin 2. *Science.* 1999;286:2495–2498.
21. Cordery SF, Husbands SM, Bailey CP, Guy RH, Delgado-Charro MB. Simultaneous transdermal delivery of buprenorphine hydrochloride and naltrexone hydrochloride by iontophoresis. *Mol Pharm.* 2019;16:2808–2816.
22. Majumdar S, Srirangam R. Solubility, stability, physicochemical characteristics and in vitro ocular tissue permeability of hesperidin: a natural bioflavonoid. *Pharm Res.* 2009;26:1217–1225.
23. Tamura G, Ichinose M, Fukuchi Y, Miyamoto T. Transdermal tulobuterol patch, a long-actingβ(2)-agonist. *Allergol Int.* 2012;61:219–229.
24. Miyano K, Sudo Y, Yokoyama A, et al. History of the G protein-coupled receptor (GPCR) assays from traditional to a state-of-the-art biosensor assay. *J Pharmacol Sci.* 2014;126:302–309.
25. Meguro Y, Miyano K, Hirayama S, et al. Neuropeptide oxytocin enhances μ opioid receptor signaling as a positive allosteric modulator. *J Pharmacol Sci.* 2018;137:67–75.
26. D'amour FE, Smith DL. A method for determining loss of pain sensation. *J Pharmacol Exp Ther*. 1941;72:74–79.
27. Cachia E, Ahmedzai SH. Transdermal opioids for cancer pain. *Curr Opin Support Palliat Care.* 2011;5:15–19.
28. Kornick CA, Santiago-Palma J, Moryl N, Payne R, Obbens EA. Benefit-risk assessment of transdermal fentanyl for the treatment of chronic pain. *Drug Saf.* 2003;26:951–973.
29. Franz TJ. Percutaneous absorption. On the relevance of in vitro data. *J Invest Dermatol*. 1975;64:190–195.
30. Azzam AAH, McDonald J, Lambert DG. Hot topics in opioid pharmacology: mixed and biased opioids. *Br J Anaesth.* 2019;122:e136–e145.
31. Raehal KM, Walker JKL, Bohn LM. Morphine side effects in β-Arrestin 2 knockout mice. *J Pharmacol Exp Ther*. 2005;314:1195–1201.
32. Maguma HT, Dewey WL, Akbarali HI. Differences in the characteristics of tolerance to μ-opioid receptor agonists in the colon from wild type and β-arrestin2 knockout mice. *Eur J Pharmacol.* 2012;685:133–140.
33. Kang M, Maguma HT, Smith TH, Ross GR, Dewey WL, Akbarali HI. The role of β-arrestin2 in the mechanism of morphine tolerance in the mouse and guinea pig gastrointestinal tract. *J Pharmacol Exp Ther.* 2012;340:567–576.
34. Chu Sin Chung P, Kieffer BL. Delta opioid receptors in brain function and diseases. *Pharmacol Ther.* 2013;140:112–120.
35. Vanderah TW. Delta and kappa opioid receptors as suitable drug targets for pain. *Clin J Pain.* 2010;26(suppl 10):S10–S15.
36. Holdridge SV, Cahill CM. Spinal administration of a delta opioid receptor agonist attenuates hyperalgesia and allodynia in a rat model of neuropathic pain. *Eur J Pain.* 2007;11:685–693.
37. Baamonde A, Lastra A, Juárez L, García V, Hidalgo A, Menéndez L. Effects of the local administration of selective mu-, delta-and kappa-opioid receptor agonists on osteosarcoma-induced hyperalgesia. *Naunyn Schmiedebergs Arch Pharmacol.* 2005;372:213–219.